Fabrication of Dye Sensitized Solar Cell (DSSC) Using Combination of Dyes Extracted from Curcuma (*Curcuma xanthorrhiza*) Rhizome and Binahong (*Anredera cordifolia*) Leaf with Treatment in pH of the Extraction

Pirim Setiarso*, Rifanda Viantiano Harsono, and Nita Kusumawati

Department of Chemistry, Faculty of Mathematics and Natural Sciences, Universitas Negeri Surabaya, Jl. Ketintang, Surabaya 60231, Indonesia

*** Corresponding author:**

email: pirimsetiarso@unesa.ac.id

Received: September 20, 2022
Accepted: June 8, 2023

DOI: 10.22146/ijc.77860

Abstract: *Research on Dye Sensitized Solar Cell (DSSC) fabrication has been carried out using a combination of dyes extracted from* Curcuma xanthorrhiza *and* Anredera cordifolia*. Each dye was extracted by treating pH 1 to 13 and then characterized using UV-Vis spectroscopy. The band gap energy was determined by using the cyclic voltammetric method. The UV-Vis spectrum of* C. xanthorrhiza *extract reveals the presence of curcumin components. The UV-Vis spectrum of* A. cordifolia *indicates the presence of chlorophyll and a trace of anthocyanin.* C. xanthorrhiza *extract had the least band gap energy in the acid phase, pH 1, at 0.66 eV, and the alkaline phase, pH 13, at 0.43 eV. The minimum band gap energy of* A. cordifolia *extract was determined to be 0.96 eV in the acid phase, pH 7, and 0.65 eV in the alkaline phase, pH 12. When* A. cordifolia *and* C. xanthorrhiza *extracts were mixed, with the best composition ratios being pH 7:pH 1 (3:2 ≈ pH 1.7) and pH 12:pH 13 (1:4 ≈ pH 12.6). The composition of this mixture was applied to the DSSC resulting in an efficiency of 0.096 and 0.147%, respectively.*

Keywords: Curcuma xanthorrhiza*;* Anredera cordifolia*; pH; extract; DSSC*

■ INTRODUCTION

The demand for energy around the world is increasing every day, and this trend will continue in the future. Therefore, efforts to develop renewable energy sources continue to be made, such as energy from the sun, wind, and water, which are widely available in nature at low cost [1-3]. This motivates researchers to explore energy sources that are clean, practical, renewable, abundant, and environmentally friendly. One of the promising renewable energy sources is solar cells, also known as photovoltaic solar cell to harvest solar energy [4]. Solar energy is one of the energies that can be converted into other energies [5-7]. Sunlight can be converted into electrical energy using solar cells by converting solar radiation directly into a source of electrical energy [8-9].

Dye Sensitized Solar Cells (DSSC) were first discovered by Michael Grätzel and Brian O'Regan in 1991. DSSC continues to develop until the manufacture of Nitrogen-doped carbon nanotubes grafting rutile TiO_2 nanofilms, which is carried out by Belkhanchi et al. [10]. The DSSC device consists of a conductive glass, a semiconductor oxide material, a dye as a photosensitizer, an electrolyte, and a counter electrode [11-12]. Currently, the most efficient dye sensitizer used for electron transfer in DSSC is a polypyridyl ruthenium(II) complex compound, with an overall photovoltaic conversion efficiency of 10% [13]. DSSC has attracted wide attention both scientifically and industrially due to their easy manufacture, low cost, versatility, and wide range of dyes [4].

The working principle of DSSC will be briefly explained as follows. Sunlight with a certain intensity can penetrate into the dye layer because the layer of conductive glass and semiconductor crystals can be easily penetrated by visible light. If the energy of the photon hits the energy gap of the dye molecule, which is the difference between the highest electron-filled

molecular orbital (HOMO) and the lowest empty molecular orbital (LUMO), the dye will absorb it, promoting one electron from HOMO to LUMO. The light energy can cause the excitation of one electron from HOMO to LUMO in the dye molecule. The excited electrons will then be injected into the conduction band of the semiconductor then collected by the conductive glass of the anode. These electrons flow towards an inert counter electrode and are collected by the conductive glass at the cathode. Then the electrons will be captured by the redox pair electrolyte and will return to the dye for regeneration [11]. An illustration of the working principle of DSSC is shown in Fig. 1.

Recently, many DSSC studies have explored sources of natural dyes as promising sensitizers. Besides being easy to obtain, natural dyes are also cheap and environmentally friendly. Natural dyes could come from plants, such as flowers, leaves, fruit, fruit skins, and vegetables. Natural pigments that have been studied to date include anthocyanins, chlorophyll, betacyanins, betaxanthins, betalains, and beta-carotene [14]. Natural dyes can be extracted directly from plants with a variety of solvents and a variety of treatments. DSSC fabricated using extracts from plants of saffron, mallow, red onion, and oregano has an efficiency of 0.51, 0.45, 0.54, and 0.51, respectively [15]. Previous studies have also reported that DSSC fabricated using extracts from pandan leaves has an efficiency of 0.35% [16] and spinach leaves of 0.002% [17].

Many studies in the world also focus research on semiconductor materials. Research on semiconductors is expected to increase the efficiency of DSSC, which also considers the dye molecules that can easily bind to the layer.

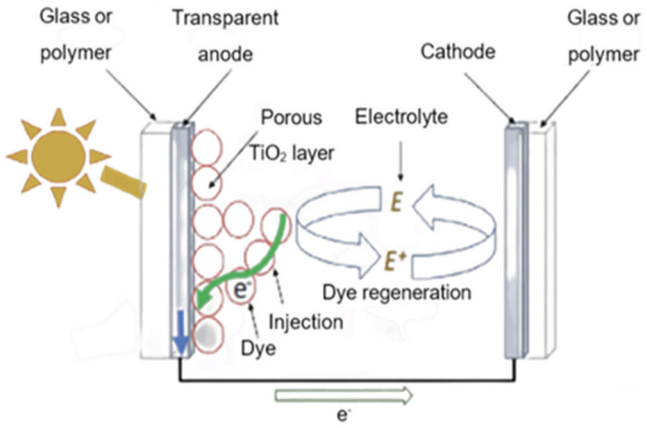

Fig 1. Working principle of DSSC [18]

Until now, the most frequently used semiconductor is TiO_2 because it is stable, easy to obtain, and non-toxic [19]. In addition, the dye can also bind easily to the TiO_2 layer to improve the performance of the DSSC. Semiconductors besides TiO_2, there are also other materials such as ZnO [20], SnO_2 [21], ZnO-CdS [22], ZnO-Fe_2O_3 [23], and TiO_2-Ag [24].

The purpose of this study was to determine the performance efficiency of DSSC using dyes extracted from *Curcuma xanthorrhiza* and *Anredera cordifolia*. Each sample was optimized for pH in the extraction process to determine the smallest band gap energy. From here, the smallest band gap will be varied in the mixing composition, and the smallest band gap energy will be sought again. Then, it will be used for DSSC fabrication. Measurement of band gap energy using Cyclic Voltammetry (CV) method, and for the characterization of compounds using UV-Vis spectrophotometry.

■ EXPERIMENTAL SECTION

Materials

TiO_2 powder obtained from Sigma Aldrich. NaOH, KI, and polyethylene glycol (PEG 1000) were purchased from Merck. Demineralization water purchased from CIMS. Ethanol and acetonitrile were purchased from Fulltime. *C. xanthorrhiza* rhizome and *A. cordifolia* leaves were bought from local markets in Pabean-Surabaya, with curcumin concentration varying from 1.0–2.4% in the extract of *C. xanthorrhiza* rhizome and chlorophyll content ranging from 20 to 24 mg/L in the extract of *A. cordifolia*. Carbon pencil 2B (Faber-Castell), Kimwipes KIMTECH (PT Indolab Utama) and cudle wax (Aladin, PT Elos Bintang Selamat). Iodine (I_2) was purchased in VWR Chemicals. ITO conductive glass was purchased from Ali Jaya Lab. HNO_3 was obtained from Emsure while HCl was purchased from SAP Chemicals.

Instrumentation

Calibrated digital pH meter (ATC), used to adjust pH. A rotary evaporator (Buchi R-300) is used to evaporate the solvent resulting from the extraction. UV-Vis spectroscopy (Shimadzu 1800) was used to

characterize the compounds produced from the extraction of *C. xanthorrhiza* and *A. cordifolia*. The band gap energy was determined using a Voltammetry (797 VA Computrace). DSSC performance test using 10-watt LED lamp (509.554 mW/cm^2), multimeter, potentiometer, and other supporting tools.

Procedure

Extraction of C. xanthorrhiza *rhizomes*

The obtained *C. xanthorrhiza* is then peeled off and washed with water until clean. *C. xanthorrhiza* that has been cleaned, cut into small pieces, and then dried using an oven. *C. xanthorrhiza* was extracted using the maceration method. The dried *C. xanthorrhiza* is reduced in size by breaking it, then macerated using ethanol with a ratio of 1:10 (sample:solvent). Optimization of the extraction is done by adjusting the pH from 1 to 13. Adjust the pH by adding HCl and NaOH. Maceration was carried out in dark conditions and protected from light for ± 24 h. The extraction results were then filtered using filter paper. The obtained filtrate is concentrated using a rotary evaporator.

Extraction of A. cordifolia *leaves*

The leaves were obtained from the *A. cordifolia* plant, which was separated from the stem. Then the *A. cordifolia* leaves were cleaned with a tissue that had been moistened with a little water and then cut into small pieces. The extraction process for *A. cordifolia* leaves was the same as for *C. xanthorrhiza* rhizomes.

Preparation of TiO_2 paste

TiO_2 paste was prepared based on the procedure from previous research [25], with a slight modification by adding PEG 1000. A 1.15 g TiO_2 powder was added with 1.5 g PEG 1000. Then 1.5 mL HNO_3 was added to the mixture and stirred for ± 30 min until evenly distributed. After that, let it stand for ± 10 min until the paste is stable.

Preparation of working electrode

The working electrode was prepared following the procedure from previous work [26], with slight modifications. The prepared TiO_2 paste was coated onto the ITO glass on the conductive side. Paste the coating using the Doctor Blade method, with an area of 2 cm × 1.5 cm. Then the glass is heated at 450 °C using a hot plate for 30 min. The sintering product is left to stand until the temperature returns to normal. TiO_2 coating that exceeds the active area of 2 cm × 1.5 cm is removed with ethanol-soaked laboratory wipes.

The finished glass is then soaked in color pigments extracted from *C. xanthorrhiza* and *A. cordifolia* for 24 h. Soaking is done in a dark place away from light. After soaking, color pigments that exceed the active area are removed with ethanol-soaked laboratory wipes.

Preparation of counter electrode

The counter electrode was made following the procedure from previous research [27], with some modifications. ITO glass was made with a deposition size of 2 cm × 1.5 cm using tape. A 2B pencil graphite is shaded on ITO glass, then the tape is removed. ITO glass which has been shaded with pencil graphite, is heated over a burning candle. After that, wait until the temperature decreases, and trim the edges using ethanol-soaked laboratory wipes.

Preparation of electrolyte

The electrolyte solution was made by dissolving 8.3 g of KI and 1.27 g of I_2 in 100 mL of ethylene glycol. To avoid direct sunlight, the solution was stored in a dark place.

Assembly of dye-sensitized solar cell

The DSSC circuit starts from the working electrode, then stacked with the opposing electrode, clamped left and right with a paperclip. After that, the electrolyte solution is dripped on the edges, occasionally opening the paper clip gap to make it easier for the electrolyte to enter it.

Characterization and measurement

The results of *A. cordifolia* and *C. xanthorrhiza* extracts which optimized for pH values, were divided into two ranges is at pH 1 to 7 (considered as the acid phase), and at pH 8 to 13 (considered as the alkaline phase). Characterization of extracted compounds using UV-Vis spectrophotometry. Then the band gap energy is determined using CV method, with a potential range of -1 to 1 V and a scan rate of 20 mV/s.

Characterization of DSSC is determined from the value of V_{oc}, I_{sc}, P_{in}, FF, and efficiency. To test the

performance of DSSC using a potentiometer 250 kΩ. For the light source, a LED lamp 10 watt is used with a light intensity of 509.554 mW/cm^2. The overall performance of the cell was determined by FF. The FF (Eq. (1)) and cell efficiency (η) (Eq. (2)) were calculated using the following formula [28];

$$FF = \frac{V_{max} \times I_{max}}{V_{oc} \times I_{sc}} \quad (1)$$

$$\eta = \frac{FF \times V_{oc} \times I_{sc}}{P_{in}} \times 100\% \quad (2)$$

where V_{max} = maximum output voltage, I_{max} = maximum output current, I_{sc} = short circuit current, V_{oc} = open circuit voltage, and P_{in} = input power 509.554 mW/cm^2.

■ RESULTS AND DISCUSSION

UV-Vis Spectroscopic Characterization of *C. xanthorrhiza*

Results of *C. xanthorrhiza* extract with pH treatment did not show a significant shift in wavelength. In the pH range of 1–7 (Fig. 2(a)), the resulting wavelength is around 424 nm. This compound tends to be stable and maintains its structure in acidic conditions [29]. A peak with a maximum wavelength of 422 nm was found at pH 8–11 (Fig. 2(b)). At pH 8–11 (Fig. 2(b)), the resulting wavelength is around 422 nm, pH 13 has shifted to 419 nm and there are signs of the appearance of small absorption at a wavelength of 438 nm. This is a characteristic of curcumins in *C. xanthorrhiza*. Electron excitation of the π→π* transition occurs in the absorption band in the visible light range, not the n→π* transition, which is proven by theoretical studies [30-31]. Although not significant, curcumin at pH 8–12 experienced a hypochromic or blue shift effect caused by the influence of solvents. At pH 13, a shoulder peak occurs at 438 nm. Alkaline hydrolysis causes the degradation of curcumin, resulting in ferulic acid and feruloyl methane fractions, which reduce absorbance [32-33]. This is supported by the research of Sinha et al. [34] and Pourhajibagher et al. [35] who reported that curcumin extracts in ethanol show variable wavelengths around 350–470 nm due to the degradation of curcumin compounds at the pH above 11.

UV-Vis Spectroscopic Characterization of *A. cordifolia*

Results of the *A. cordifolia* extract will be presented in this study. Treatment of pH extract under acidic conditions did not show a significant wavelength shift. It can be seen in Fig. 3(a), the treatment of pH 1–7 on the extract showed the same peak pattern. The absorption peaks appear at 664, 436, and 412 nm, which reflect the characteristics of the chlorophyll a [35-36]. Theoretically, chlorophyll will lose the central magnesium atom in its structure under acidic conditions, which is called pheophytin. The green color has faded, turning yellow [37-38]. From the spectrum in Fig. 3(a), it can be predicted that the presence of chlorophyll a that lost a central magnesium atom is called pheophytin a because

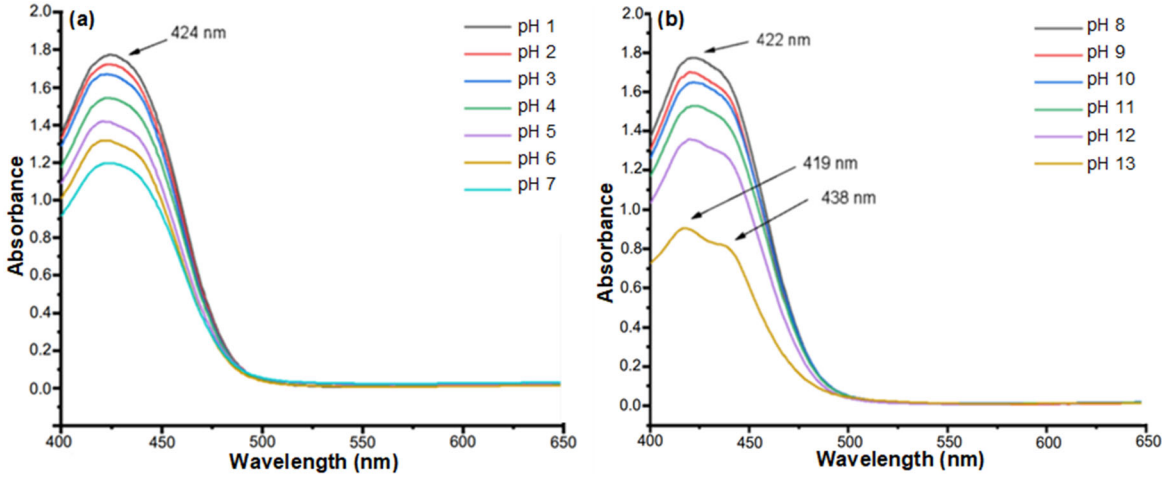

Fig 2. The spectrum of *C. xanthorrhiza* extract (a) pH 1 to 7 and (b) pH 8 to 13

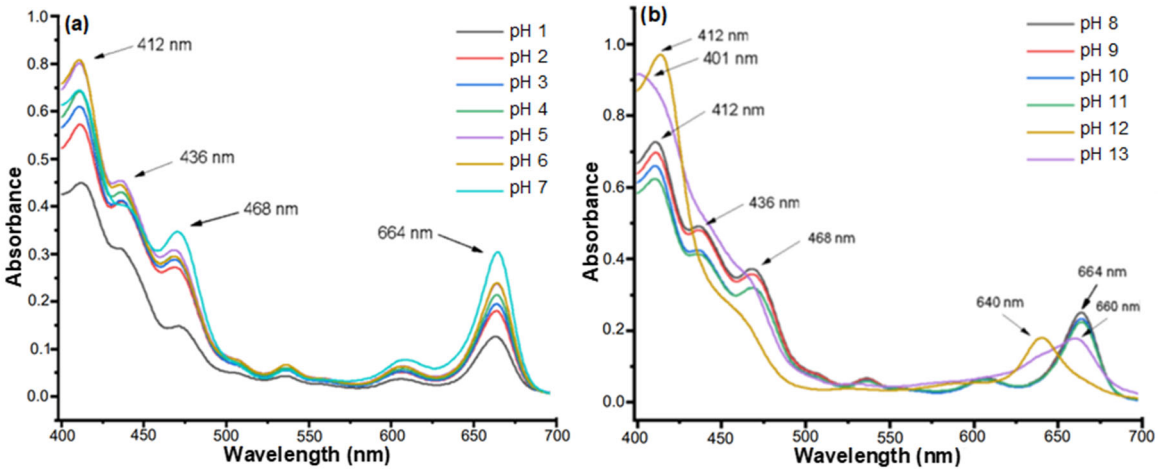

Fig 3. The spectrum of *A. cordifolia* extract (a) pH 1 to 7 and (b) pH 8 to 13

chlorophyll a absorbs red light at approximately 662 nm and violet light at approximately 430 nm. Then the absorption peak appears at 468 nm, which indicates the presence of anthocyanin molecules [39]. However, the treatment of pH 1–7 affects the absorbance. Where the increase in pH from 1 to 7, the absorbance also increases. The increase in absorbance is related to the number of molecules or the concentration of chlorophyll a that has been extracted. Then it can be seen in Fig. 3(b), there is no shift in wavelength at pH 8–11. The absorption pattern is still the same with pH 1–7. However, there was a decrease in absorbance at pH 8–11. This is related to the quantity of molecules or the concentration of chlorophyll a that is extracted less. At pH 12 there is a change in the wavelength absorption. The resulting wavelengths are 640 and 412 nm. Predictably this absorption is an intact chlorophyll b with a central magnesium atom. At pH 12 there was also no absorption peak at a wavelength of 468 nm, which indicated that anthocyanin compounds were not extracted at this pH. At pH 13, the resulting wavelengths are 660 and 401 nm. There is a shift of 664 to 660 nm. Predictably at the top is the presence of an intact chlorophyll a with magnesium as the central atom. Besides that, there is a shift in the absorption of the wavelength at the peak of 412 to 401 nm. This is related to the chlorophyll a which is hydrolyzed into chlorophyllide a and phytol group [40-41].

Band Gap Determined of Cyclic Voltammetry

The band gap energy of the extraction results with pH treatment was determined by the CV method. Measurements were made at a scan rate of 20 mV/s at a potential range of −1 to 1 V. The band gap energy was determined from the difference between HOMO and LUMO values. If the difference between the HOMO and LUMO values is getting smaller, the better the quality of the extracted dye. The ability to regenerate dyes shows the ease of electron transfer from electrolyte I^-/I_3^- to the HOMO band of the substance. This is related to the easier process of excitation of dye electrons from the valence band to the conduction band; with sufficiently small energy, the electrons can be excited. The conduction band is affected by the TiO_2; which the effect of TiO_2 will be in line with the energy of the LUMO dye compound, the easier it is for electron injection. The values calculated in the equation below involve 4.40 eV as the standard energy level of iodine electrolyte below the vacuum level (b). Thus, the HOMO, LUMO, and band gap energy values can be calculated by Eq. (3-5) [42].

$$E_{HOMO} = -e\left(E_{ox} + 4.40\right)eV \quad (3)$$

$$E_{LUMO} = -e\left(E_{red} + 4.40\right)eV \quad (4)$$

$$E_g = E_{LUMO} - E_{HOMO} \quad (5)$$

The HOMO value is correlated with the oxidation state (oxidation peak), while the LUMO is correlated with the reduction state (reduction peak) of the CV [34]. The CV can be seen in Fig. 4. This research will study the combination of dye mixtures and compositions. The band gap energy values are summarized in Table 1. In the range of pH 1 to 7, the best band gap energy of *C.*

xanthorrhiza extract was at pH 1 of 0.66 eV. While in the pH range 1 to 7, the best band gap energy is found at pH 7 of 0.96 V. The *A. cordifolia* extract in the range of pH 8 to 13 has the best band gap energy at pH 13 of 0.43 eV. Meanwhile, in the range of pH 8 to 13, the best band gap energy at pH 12 is 0.65 eV. Of all the dye extraction results with pH variations that have been described, all of them have the potential to become sensitizers in DSSC. However, the band gap energy is taken from this optimum pH to be used for mixing variations. Characterization was also carried out by UV-Vis spectroscopy and voltammetry. The bandgap energy of TiO_2 is 3.2 eV [43]. The LUMO TiO_2 energy has been determined to be −4.00 eV [44]. So that the excitation of electrons from the dye will be easier to inject into the TiO_2 layer when exposed to light. Therefore, the dye produced in this study has the potential as a DSSC sensitizer and is expected to increase DSSC efficiency. Electrons are injected into the conduction band of the porous semiconductor layer because the LUMO of the dye has a higher energy level than that of the conduction layer. Suggesting that the electron injection from these LUMOs to the TiO_2 conduction band is possible. Use of TiO_2 for a variety of benefits, including it is stable, can be used as an electrode in photoelectrochemical systems operating at high temperatures, is inexpensive, non-toxic, and has good optical properties that aid the injection of excited dye electrons into the semiconductor [44].

UV-Vis Spectroscopic Characterization of Mixed Extracts

This characterization is viewed from the best band gap energy determined by the previous CV method. In this study, the extract was mixed in two parts, acid and alkaline. Under acidic conditions, the extracts of pH 7 and 1 were mixed, while in alkaline conditions, the extracts

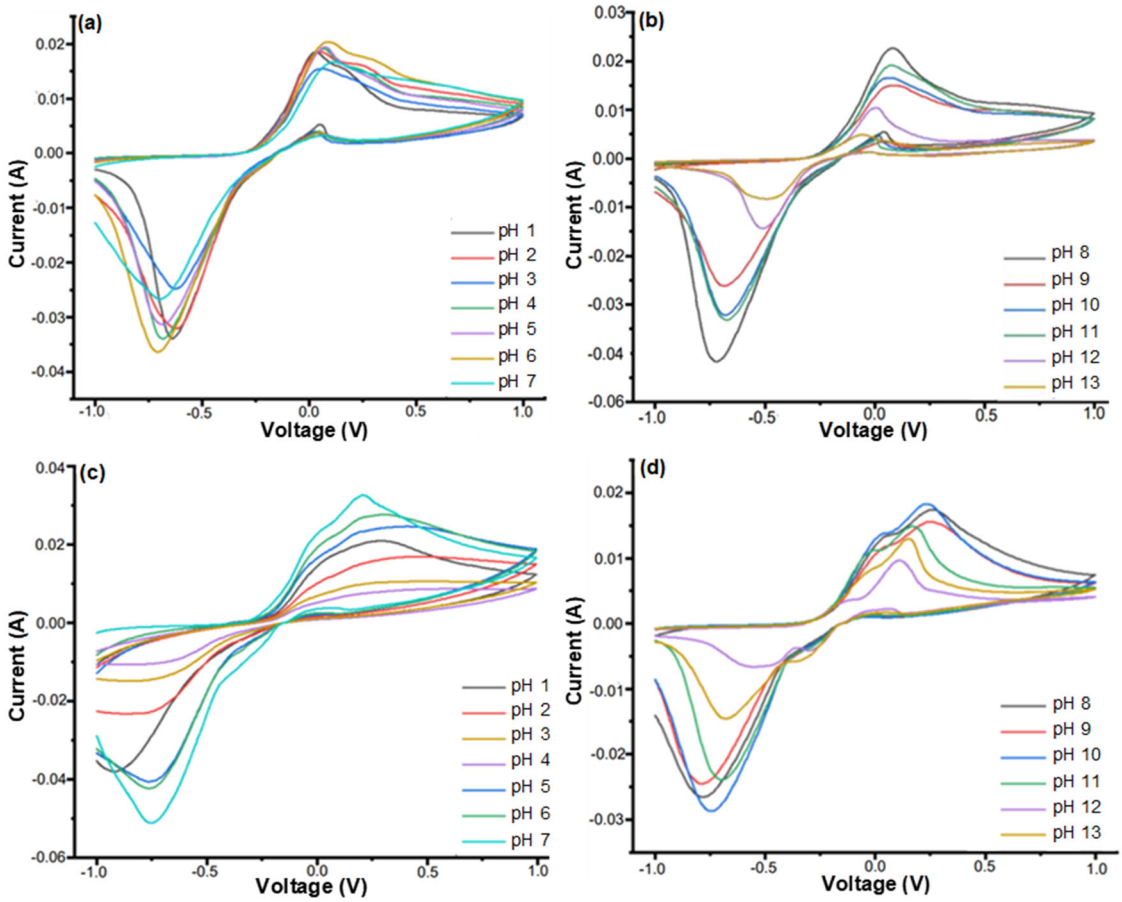

Fig 4. Cyclic voltammogram of *C. xanthorrhiza* extract (a) pH 1 to 7 (b) pH 8 to 13, and *A. cordifolia* extract (c) pH 1 to 7, (d) pH 8 to 13

Table 1. Energy band gap between HOMO and LUMO, extraction results with variations in pH

pH	*C. xanthorrhiza* extract			*A. cordifolia* extract		
	HOMO (eV)	LUMO (eV)	Band gap (eV)	HOMO (eV)	LUMO (eV)	Band gap (eV)
1	-4.42	-3.76	0.66	-4.69	-3.48	1.21
2	-4.45	-3.78	0.67	-4.69	-3.65	1.04
3	-4.46	-3.78	0.68	-4.67	-3.64	1.03
4	-4.46	-3.71	0.75	-4.66	-3.64	1.02
5	-4.47	-3.71	0.76	-4.69	-3.70	0.99
6	-4.48	-3.69	0.79	-4.61	-3.63	0.98
7	-4.51	-3.70	0.81	-4.60	-3.64	0.96
8	-4.48	-3.68	0.80	-4.66	-3.62	1.04
9	-4.48	-3.72	0.76	-4.65	-3.62	1.03
10	-4.47	-3.72	0.75	-4.63	-3.66	0.97
11	-4.47	-3.72	0.75	-4.57	-3.70	0.87
12	-4.41	-3.89	0.52	-4.50	-3.85	0.65
13	-4.34	-3.91	0.43	-4.49	-3.83	0.66

were mixed with pH 12 and 13. The mixture was varied in the composition ratio of 1:4, 2:3, 1:1, 3:2, and 4:1 (*A. cordifolia* extract: *C. xanthorrhiza* extract).

The results of mixing extract pH 7 and 1 with a composition ratio of 1:4, 2:3, 1:1, 3:2, and 4:1 resulted in the final pH being 1.2, 1.5, 1.6, 1.7, and 2.0. UV-Vis spectrum resulting from a mixture of pH 7 and 1 with various composition ratios can be seen in Fig. 5. The spectrum which is generated from the entire composition mixture shows the dominance of curcumin molecules. The resulting absorption peak is 423 nm, and for a mixture of 4:1, composition is 422 nm. Almost no visible signs of the presence of chlorophyll molecules. This is because the ethanol solvent does show a more suitable level of polarity in the curcumin molecule than in chlorophyll. Basically, the curcumin molecule produces a higher concentration when extracted using ethanol than chlorophyll. Chlorophyll has a side chain called phytol in which there are many methyl functional groups, thus reducing the polarity when extraction using ethanol solvent. If seen, indeed, the curcumin molecule produces a relatively higher absorbance in the previous characterization than chlorophyll.

The results of mixing extract pH 12 and 13 with a composition ratio of 1:4, 2:3, 1:1, 3:2, and 4:1 resulted in the final pH is 12.6, 12.4, 12.3, 12.2, and 12.1. UV-Vis spectrum

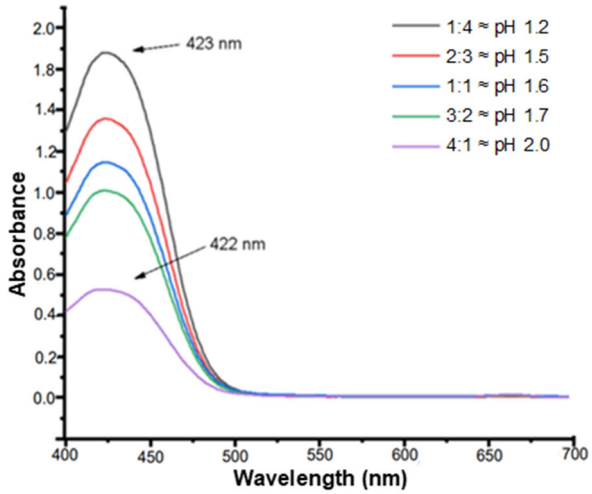

Fig 5. UV-Vis spectrum mixture composition *A. cordifolia* pH 7 and *C. xanthorrhiza* pH 1

resulting from a mixture of pH 12 and 13 with various composition ratios can be seen in Fig. 6. The spectrum which resulted is still the same as before, namely the dominance of curcumin molecules and no signs of the presence of chlorophyll molecules. A mixture of 1:4 composition resulted in a strong peak at 417 nm and a shoulder peak at 439 nm. At a mixture of 2:3 and 1:1 composition, it resulted in a strong peak at 417 nm and a broad peak at 438 nm. Then a mixture of 3:2 composition resulted in an absorption peak at 419 nm, and no shoulder peak appeared as in the previous

composition. Finally, the 4:1 composition mixture only produces an absorption peak at 417 nm, and the shoulder peak that appears is not too strong and sharp. This shows that the composition mixture only shifts the absorption peak slightly so that it experiences a bathochromic effect on the shoulder peak and a hypochromic effect on the strong peak.

Determination Band Gap of Mixed Extracts

This characterization is based on the best band gap energy determined by the previous CV method on each dye that has the best pH for acidic and alkaline conditions. In acidic conditions, *A. cordifolia* extract with pH 7 and *C. xanthorrhiza* extract with pH 1 were combined, while in alkaline conditions, *A. cordifolia* extract with pH 12 was combined with *C. xanthorrhiza* extract with pH 13. Each of these combinations varied with composition ratios of 1:4, 2:3, 1:1, 3:2, and 4:1 (*A. cordifolia* extract: *C. xanthorrhiza* extract). The CV can be seen in Fig. 7.

In a mixture of extracts pH 7 and 1, the best band gap was obtained at a composition of 3:2 with a final pH of 1.7. pH 1.7 is the most optimal concentration in the extract mixture. This is because at this pH, it has the lowest band gap among the other mixtures, as shown in Table 2. The smaller the band gap in the mixture, the easier the dye electron excitation process from the valence band to the conduction band will be, so the quality of the mixed dye will be better. When exposed to light, the electrons will be excited properly and consequently inject into the TiO_2 layer. Higher concentration could cause an obstacle to the total electron excitation process, so the excitation does not take place optimally.

The results of measurements of HOMO-LUMO energy and energy band gap *A. cordifolia* extract mixture (pH 7) and *C. xanthorrhiza* extract (pH 1) as well as a mixture of *A. cordifolia* extract (pH 12) and *C. xanthorrhiza* extract (pH 13) were determined by voltammetry can be seen in Tables 2 and 3.

The best bandgap composition in the mixed extract pH 12 and 13, a composition of 1:4, was found with a final pH of 12.6. The molecular concentration at pH 12.6 is considered the most optimal. The curcumin molecules extracted at pH 13 were less, therefore the composition

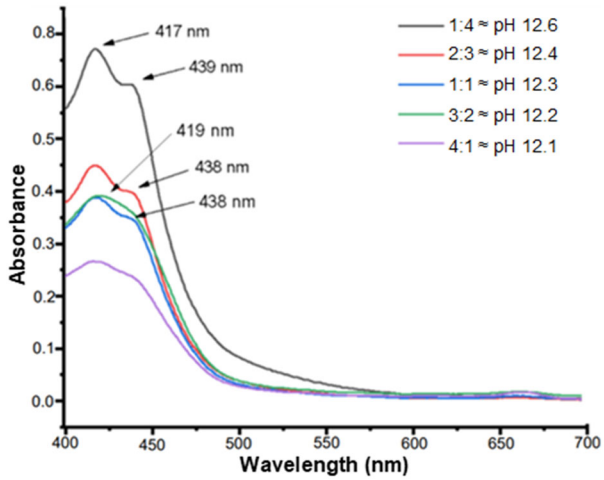

Fig 6. UV-Vis spectrum mixture composition *A. cordifolia* pH 12 and *C. xanthorrhiza* pH 13

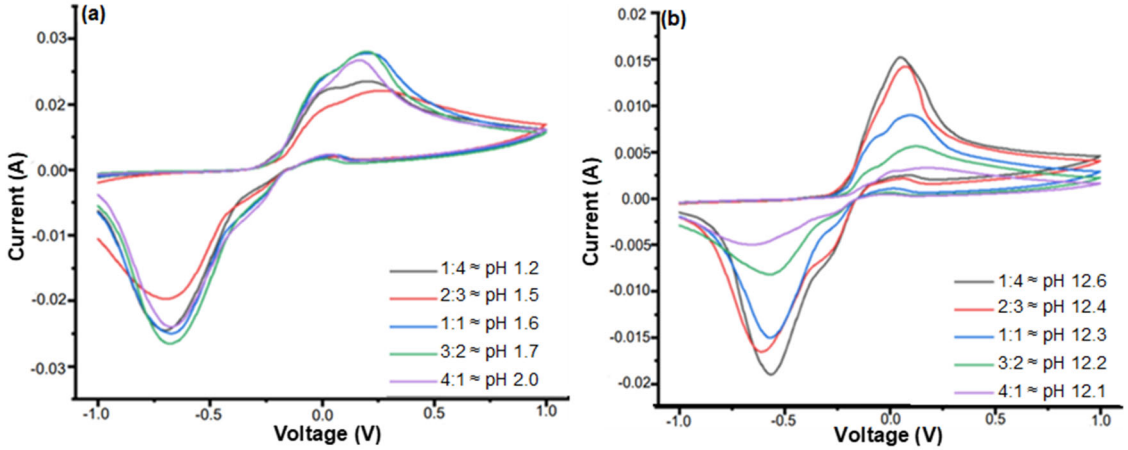

Fig 7. Cyclic voltammogram mixture composition (a) *A. cordifolia* pH 7 and *C. xanthorrhiza* pH 1 (b) *A. cordifolia* pH 12 and *C. xanthorrhiza* pH 13

Table 2. HOMO, LUMO, and band gap mixture pH 7 and 1

Mixture composition	Mixture of *A. cordifolia* extract (pH 7) and *C. xanthorrhiza* extract (pH 1)		
	HOMO (eV)	LUMO (eV)	Band gap (eV)
1:4 ≈ pH 1.2	-3.70	-4.60	0.90
2:3 ≈ pH 1.5	-3.70	-4.66	0.96
1:1 ≈ pH 1.6	-3.73	-4.60	0.87
3:2 ≈ pH 1.7	-3.73	-4.57	0.84
4:1 ≈ pH 2.0	-3.72	-4.60	0.88

Table 3. HOMO, LUMO, and band gap mixture pH 12 and pH 13

Mixture composition	Mixture of *A. cordifolia* extract (pH 12) and *C. xanthorrhiza* extract (pH 13)		
	HOMO (eV)	LUMO (eV)	Band gap (eV)
1:4 ≈ pH 12.6	-3.83	-4.45	0.62
2:3 ≈ pH 12.4	-3.79	-4.47	0.68
1:1 ≈ pH 12.3	-3.83	-4.50	0.67
3:2 ≈ pH 12.2	-3.73	-4.57	0.69
4:1 ≈ pH 12.1	-3.74	-4.58	0.84

of the mixture at pH 12.6 was more abundant than *C. xanthorrhiza* extract. The composition ratio between chlorophyll b and curcumin molecules is optimum in this composition because it has a smaller band gap than *C. xanthorrhiza* extract or *A. cordifolia* extract. In a mixture of these compositions, both can excite electrons well when exposed to light.

DSSC Performance Sensitized from Mixture Selected Compositions of Dyes

DSSC performance was tested using a 10-watt LED lamp with a light intensity of 509.554 mW/cm^2. The distance between the lamp and the DSSC is 4 cm. Measurement of DSSC performance using a potentiometer as reported by Setyawati et al. [45]. Characterization includes V_{oc}, I_{sc}, Fill Factor, and efficiency. The summary and characterization of the I-V curve of the DSSC can be seen in Table 4 and Fig. 8.

In this study, a mixture of pH 7 and 1 extracts was selected at a ratio of 3:2 with a pH of 1.7. This combination resulted in cell parameters of I_{sc} = 2.5 μA, V_{oc} = 320 mV, and FF = 1.83, with a maximum cell efficiency of 0.096%. Under acidic conditions, curcumin molecules tend to be stable and maintain their structure. However, in the extraction process, the pH treatment affected the concentration of the extracted curcumin molecules, so the best was chosen [46]. Meanwhile, chlorophyll in acidic conditions affects the release of a magnesium atom as the central atom of the chlorophyll complex. In addition, the presence of anthocyanins was detected at this pH when extracted. This is associated with the greater steric hindrance when mixing, which will affect the binding to the TiO_2 layer, and also the injection of electrons into the TiO_2 layer when exposed to light. The structure of the anthocyanins may influence DSSC performance. For example, if the structure includes

Table 4. Characterization DSSC mixture of the best composition *A. cordifolia* extract and *C. xanthorrhiza* extract

Extract mixture (pH)	Composition ratio	V_{oc} (mV)	I_{sc} (μA)	FF	Efficiency (%)
7 and 1	3:2 ≈ pH 1.7	320	2.5	1.83	0.096
12 and 13	1:4 ≈ pH 12.6	407	3.3	1.67	0.146

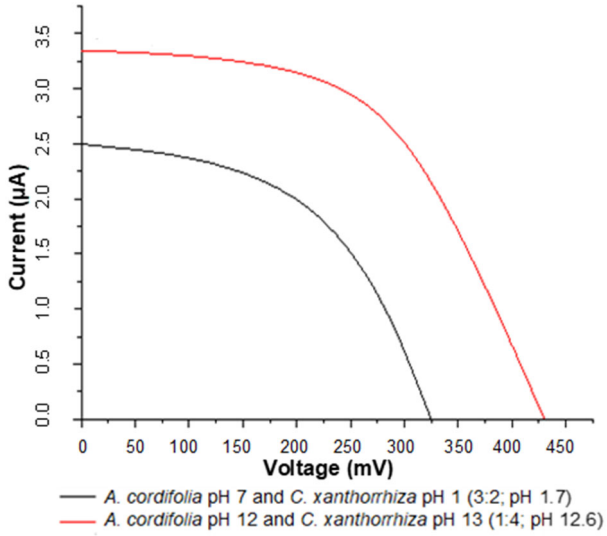

Fig 8. I-V Curves DSSC mixture of the best composition *A. cordifolia* extract and *C. xanthorrhiza* extract

a longer R group, the steric hindrance for the anthocyanin to form a bond with the oxide surface of the TiO_2. As a result, it efficiently blocks the molecule from chemical adsorption on the TiO_2 film layer. Therefore, in this study, the best pH was also selected, and the best mixture composition was also selected to produce optimal efficiency when used as a dye sensitizer in DSSC.

Under alkaline conditions, a mixture of pH 12 and 13 was chosen with a ratio of 1:4 to produce a final pH of 12.6, to be used as a dye sensitizer in DSSC. In the alkaline phase, curcumin molecules have hydrolysis so that they are degraded. This causes a change in the chromophore group, which results in a change in visible light absorption, resulting in a smaller band gap for electron excitation. Then chlorophyll at this pH is predicted as pure chlorophyll without anthocyanins, and also, the central magnesium atom cannot be separated. So that when mixing, the steric resistance that occurs is smaller than that of the acidic phase. This makes the process of chemical bonding by the dye functional groups to the TiO_2 layer easier, and also, when exposed to light, it will be easier to inject electrons into the TiO_2 layer. At this stage, the selection of the best composition is also carried out to obtain optimal efficiency and sensitivity to sunlight. In alkaline conditions, the best combination of *A. cordifolia* extract pH 12 with *C. xanthorrhiza* extract pH 13 is a ratio of 1:4 with a final pH of 12.6. The composition of this combination has the smallest band gap energy that has been determined by cyclic voltammetry and also characterized using UV-Vis spectroscopy. The observed cell parameters from this combination were I_{sc} = 3.3 μA, V_{oc} = 407 mV, and FF = 1.67, with the maximum cell efficiency obtained being 0.146%.

■ CONCLUSION

Sensitized DSSC from extracts of *C. xanthorrhiza* and *A. cordifolia* with pH treatment has been successfully fabricated. The UV-Vis spectrum shows that the extracted pigment contains curcumin and chlorophyll compounds. The pH treatment also showed a shift in the characteristics of the absorption peak associated with changes in the chromophore and auxochrome groups in the molecule. The band gap energy of the extracted dye, by pH treatment, was determined using cyclic voltammetry. These two dyes have the potential to be applied as DSSC sensitizers. The best mixture of these two dyes (*A. cordifolia* extract:*C. xanthorrhiza* extract) was found at pH 7 and 1 with a composition of 3:2 ≈ pH 1.7, producing V_{oc}, I_{sc}, FF, and η, of 320 mV, 2.5 μA, 1.83, and 0.096%, respectively. Then at pH 12 and 13 with a composition of 1:4 ≈ pH 12.6, it produced V_{oc}, I_{sc}, FF, and η, of 407 mV, 3.3 μA, 1.67, and 0.146%, respectively.

■ AUTHOR CONTRIBUTIONS

Rifanda Viantiano Harsono and Pirim Setiarso contributed to the extraction of curcuma rhizome and binahong leaves as well as the fabrication of DSSC. Nita Kusumawati contributed to the UV-Vis analysis. In addition, this article manuscript was written by all authors.

■ REFERENCES

[1] Mamur, H., Dilmaç, Ö.F., Begum, J., and Bhuiyan, M.R.A., 2021, Thermoelectric generators act as renewable energy sources, *Cleaner Mater.*, 2, 100030.

[2] Silva, N., Fuinhas, J. A., and Koengkan, M., 2021, Assessing the advancement of new renewable energy sources in Latin American and Caribbean countries, *Energy*, 237, 121611.

[3] Dong, F.Y., Xu, S., Guo, W., Jiang, N.R., Han, D.D., He, X.Y., Zhang, L., Wang, Z.J., Feng, J., Su, W., and Sun, H.B., 2020, Solar-energy camouflage coating with varying sheet resistance, *Nano Energy*, 77, 105095.

[4] Ndeze, U.I., Aidan, J., Ezike, S.C., and Wansah, J.F., 2021, Comparative performances of nature-based dyes extracted from Baobab and Shea leaves photo-sensitizers for dye-sensitized solar cells (DSSCs), *Curr. Res. Green Sustainable Chem.*, 4, 100105.

[5] Nan, H., Shen, H.P., Wang, G., Xie, S.D., Yang, G.J., and Lin, H., 2017, Studies on the optical and photoelectric properties of anthocyanin and chlorophyll as natural co-sensitizers in dye sensitized solar cell, *Opt. Mater.*, 73, 172–178.

[6] Behar, O., Peña, R., Kouro, S., Kracht, W., Fuentealba, E., Moran, L., and Sbarbaro, D., 2021, The use of solar energy in the copper mining processes: A comprehensive review, *Cleaner Eng. Technol.*, 4, 100259.

[7] Tsvetkov, N.A., Krivoshein, U.O., Tolstykh, A.V., Khutornoi, A.N., and Boldyryev, S., 2020, The calculation of solar energy used by hot water systems in permafrost region: An experimental case study for Yakutia, *Energy*, 210, 118577.

[8] Damayanti, R., Hardeli, H., and Sanjaya, H., 2014, Preparasi dye sensitized solar cell (DSSC) menggunakan ekstrak antosianin ubi jalar ungu (*Ipomea batatas* L.), *Sainstek: J. Sains Teknol.*, 6 (2), 148–157.

[9] Khan, M.I., Farooq, W.A., Saleem, M., Bhatti, K.A., Atif, M., and Hanif, A., 2019, Phase change, band gap energy and electrical resistivity of Mg doped TiO_2 multilayer thin films for dye sensitized solar cells applications, *Ceram. Int.*, 45 (17, Part A), 21436–21439.

[10] Belkhanchi, H., Ziat, Y., Hammi, M., Laghlimi, C., Moutcine, A., Benyounes, A., and Kzaiber, F., 2021, Nitrogen doped carbon nanotubes grafted TiO_2 rutile nanofilms: Promising material for dye sensitized solar cell application, *Optik*, 229, 166234.

[11] Job, F., Mathew, S., Rajendran, R., Meyer, T., and Narbey, S., 2020, An investigation on the performance of dye-sensitized solar cell at various light intensities, *Mater. Today: Proc.*, 43, 3386–3390.

[12] Güzel, R., Yediyıldız, F., Ocak, Y.S., Yılmaz, F., Ersöz, A., and Say, R., 2020, Photosystem (PSII)-based hybrid nanococktails for the fabrication of BIO-DSSC and photo-induced memory device, *J. Photochem. Photobiol., A*, 401, 112743.

[13] Bej, S., Ghosh, P., Majumdar, G., Murmu, N.C., and Banerjee, P., 2020, "Design and Synthesis of New Ruthenium Coordination Complex as Efficient Dye in DSSC Like Alternative Energy Resources with a Bird's Eye View on Strategies Towards GHGs Mitigation" in *Encyclopedia of Renewable and Sustainable Materials*, Eds. Hashmi, S., and Choudhury, I.A., Elsevier, Oxford, UK, 395–410.

[14] Wang, X.F., and Kitao, O., 2012, Natural chlorophyll-related porphyrins and chlorins for dye-sensitized solar cells, *Molecules*, 17 (4), 4484–4497.

[15] Jalali, T., Arkian, P., Golshan, M., Jalali, M., and Osfouri, S., 2020, Performance evaluation of natural native dyes as photosensitizer in dye-sensitized solar cells, *Opt. Mater.*, 110, 110441.

[16] Siddick, S.Z., Lai, C.W., and Juan, J.C., 2018, An investigation of the dye-sensitized solar cell performance using graphene-titania (TrGO) photoanode with conventional dye and natural green chlorophyll dye, *Mater. Sci. Semicond. Process.*, 74, 267–276.

[17] Rahul, R., Singh, S., Singh, P.K., Kakroo, S., Hachim, D.M., Dhapola, P.S., and Khan, Z.H., 2021, Eco-friendly dye sensitized solar cell using natural dye with solid polymer electrolyte as hole transport material, *Mater. Today: Proc.*, 34, 760–766.

[18] Cruz, H., Pinto, A.L., Lima, J.C., Branco, L.C., and Gago, S., 2020, Application of polyoxometalate-ionic liquids (POM-ILs) in dye-sensitized solar cells (DSSCs), *Mater. Lett.: X*, 6, 100033.

[19] Kishore Kumar, D., Kříž, J., Bennett, N., Chen, B., Upadhayaya, H., Reddy, K.R., and Sadhu, V., 2020, Functionalized metal oxide nanoparticles for efficient dye-sensitized solar cells (DSSCs): A review, *Mater. Sci. Energy Technol.*, 3, 472–481.

[20] Sakai, N., Miyasaka, T., and Murakami, T.N., 2013, Efficiency enhancement of ZnO-based dye-sensitized solar cells by low-temperature $TiCl_4$ treatment and dye optimization, *J. Phys. Chem. C*, 117 (21), 10949–10956.

[21] Pari, B., Chidambaram, S., Kasi, N., and Muthusamy, S., 2014, Recent advances in SnO_2 based photo anode materials for third generation photovoltaics, *Mater. Sci. Forum*, 771, 25–38.

[22] Ansir, R., Shah, S.M., Ullah, N., and Hussain, M.N., 2020, Performance of pyrocatechol violet and carminic acid sensitized ZnO/CdS nanostructured photoactive materials for dye sensitized solar cell, *Solid-State Electron.*, 172, 107886.

[23] Sebehanie, K.G., 2017, Comparative study of ZnO/Fe_2O_3 nanocomposite sensitized with natural pigments for dye sensitized solar cell, *Int. J. Hybrid Inf. Technol.*, 10 (1), 199–214.

[24] Ibrayev, N., Serikov, T., Zavgorodniy, A., and Sadykova, A., 2018, The effect of the DSSC photoanode area based on TiO_2/Ag on the conversion efficiency of solar energy into electrical energy, *IOP Conf. Ser.: Mater. Sci. Eng.*, 289, 012024.

[25] Mensah-Darkwa, K., Agyemang, F.O., Yeboah, D., and Akromah, S., 2020, Dye-sensitized solar cells based on graphene oxide and natural plant dye extract, *Mater. Today: Proc.*, 38, 514–521.

[26] Syafinar, R., Gomesh, N., Irwanto, M., Fareq, M., and Irwan, Y.M., 2015, Chlorophyll pigments as nature based dye for dye-sensitized solar cell (DSSC), *Energy Procedia*, 79, 896–902.

[27] Hölscher, F., Trümper, P., Juhász Junger, I., Schwenzfeier-Hellkamp, E., and Ehrmann, A., 2019, Application methods for graphite as catalyzer in dye-sensitized solar cells, *Optik*, 178, 1276–1279.

[28] Narasimha Rao, B., Padma Suvarna, R., Giribabu, L., Raghavender, M., and Ramesh Kumar, V., 2018, PEO based polymer composite with added acetamide, NaI/I_2 as gel polymer electrolyte for dye sensitized solar cell applications, *IOP Conf. Ser.: Mater. Sci. Eng.*, 310, 012012.

[29] Yoon, S.J., Lim, I., Kim, J.H., Adhikari, S., Lee, W.Y., Lee, J.K., Shrestha, N.K., Ahn, H., Han, J.W., and Han, S.H., 2016, Deprotonated curcumin as a simple and quick available natural dye for dye sensitized solar cells, *Energy Sources, Part A*, 38 (2), 183–189.

[30] Zsila, F., Bikádi, Z., and Simonyi, M., 2003, Molecular basis of the Cotton effects induced by the binding of curcumin to human serum albumin, *Tetrahedron: Asymmetry*, 14 (16), 2433–2444.

[31] Kim, H.J., Kim, D.J., Karthick, S.N., Hemalatha, K.V., Justin Raj, C., Ok, S., and Choe, Y., 2013, Curcumin dye extracted from *Curcuma longa* L. used as sensitizers for efficient dye-sensitized solar cells, *Int. J. Electrochem. Sci.*, 8 (6), 8320–8328.

[32] Leung, M.H.M., Colangelo, H., and Kee, T.W., 2008, Encapsulation of curcumin in cationic micelles suppresses alkaline hydrolysis, *Langmuir*, 24 (11), 5672–5675.

[33] Wang, Y.J., Pan, M.H., Cheng, A.L., Lin, L.I., Ho, Y.S., Hsieh, C.Y., and Lin, J.K., 1997, Stability of curcumin in buffer solutions and characterization of its degradation products, *J. Pharm. Biomed. Anal.*, 15 (12), 1867–1876

[34] Sinha, D., De, D., and Ayaz, A., 2018, Performance and stability analysis of curcumin dye as a photo sensitizer used in nanostructured ZnO based DSSC, *Spectrochim. Acta, Part A*, 193, 467–474.

[35] Pourhajibagher, M., Plotino, G., Chiniforush, N., and Bahador, A., 2020, Dual wavelength irradiation antimicrobial photodynamic therapy using indocyanine green and metformin doped with nano-curcumin as an efficient adjunctive endodontic treatment modality, *Photodiagn. Photodyn. Ther.*, 29, 101628.

[36] Al-Alwani, M.A.M., Ludin, N.A., Mohamad, A.B., Kadhum, A.A.H., and Sopian, K., 2017, Extraction, preparation and application of pigments from *Cordyline fruticosa* and *Hylocereus polyrhizus* as sensitizers for dye-sensitized solar cells, *Spectrochim. Acta, Part A*, 179, 23–31.

[37] Yang, M., Zhu, S., Jiao, B., Duan, M., Meng, Q., Ma, N., and Lv, W., 2020, SlSGRL, a tomato SGR-like protein, promotes chlorophyll degradation downstream of the ABA signaling pathway, *Plant*

Physiol. Biochem., 157, 316–327.

[38] Heaton, J.W., and Marangoni, A.G., 1996, Chlorophyll degradation in processed foods and senescent plant tissues, *Trends Food Sci. Technol.*, 7 (1), 8–15.

[39] Hosseinnezhad, M., Rouhani, S., and Gharanjig, K., 2018, Extraction and application of natural pigments for fabrication of green dye-sensitized solar cells, *Opto-Electron. Rev.*, 26 (2), 165–171.

[40] Kaewsuksaeng, S., 2011, Chlorophyll degradation in horticultural crops, *Walailak J. Sci. Technol.*, 8 (1), 9–19.

[41] Hörtensteiner, S., and Kräutler, B., 2000, Chlorophyll breakdown in oilseed rape, *Photosynth. Res.*, 64 (2), 137–146.

[42] Çakar, S., Atacan, K., and Güy, N., 2019, Synthesis and characterizations of TiO_2/Ag photoanodes for used indigo carmine sensitizer based solar cells, *Celal Bayar Univ. J. Sci.*, 15 (1), 23–29.

[43] Onah, E.O., Offiah, S.U., Chime, U.K., Whyte, G.M., Obodo, R.M., Ekechukwu, O.V., Ahmad, I., Ugwuoke, P.E., and Ezema, F.I., 2020, Comparative photo-response performances of dye sensitized solar cells using dyes from selected plants, *Surf. Interfaces*, 20, 100619.

[44] Hayat, A., Shivashimpi, G.M., Nishimura, T., Fujikawa, N., Ogomi, Y., Yamaguchi, Y., Pandey, S.S., Ma, T., and Hayase, S., 2015, Dye-sensitized solar cells based on axially ligated phosphorus-phthalocyanine dyes, *Appl. Phys. Express*, 8 (4), 047001.

[45] Setyawati, H., Darmokoesoemo, H., Ningtyas, A.T.A., Kadmi, Y., Elmsellem, H., and Kusuma, H.S., 2017, Effect of metal ion Fe(III) on the performance of chlorophyll as photosensitizers on dye sensitized solar cell, *Results Phys.*, 7, 2907–2918.

[46] Ramirez-Perez, J., Maria, C., and Santacruz, C.P., 2019, Impact of solvents on the extraction and purification of vegetable dyes onto the efficiency for dye-sensitized solar cells, *Renewables: Wind, Water, Solar*, 6 (1), 1.